Ubiquitin Recognition by the DNA Repair Protein hHR23a†

Qinghua Wang,‡ Amanda M. Goh,§ Peter M. Howley,§ and Kylie J. Walters*,‡

Department of Biochemistry, Molecular Biology and Biophysics, University of Minnesota, Minneapolis, Minnesota 55455, and Department of Pathology, Harvard Medical School, Boston, Massachusetts 02115

Received August 5, 2003; Revised Manuscript Received September 22, 2003

ABSTRACT: Ubiquitin is a prominent regulatory protein in numerous biological processes, including targeted protein degradation, endocytic sorting, transcriptional control, intranuclear localization, and retroviral virion budding. Ubiquitin-associated (UBA) domains, ubiquitin interacting motifs (UIM), and coupling of ubiquitin conjugation to ER degradation (CUE) motifs have been identified as ubiquitin receptors. The DNA repair protein hHR23a has two UBA domains that can each bind ubiquitin in addition to an N-terminal UBL domain that binds S5a and S2, two components of the 26S proteasome. Here we reveal hHR23a recognizes ubiquitin through a predominately hydrophobic surface formed by residues within α1 and α3 of each of its UBA domains. These two UBA surfaces bind a region on ubiquitin that includes K48. These findings have implications for published studies revealing that hHR23a inhibits K48-linked polyubiquitin chain formation. In addition, by using ^{15}N NMR relaxation experiments, we find that binding ubiquitin requires a structural change in hHR23a. HHR23 proteins are hypothesized to link ubiquitin to S5a, and we provide direct evidence that hHR23 could form a ternary complex with ubiquitin and S5a.

Ubiquitin first attracted attention, and is so named, because of its cellular abundance. This 76-residue protein is highly conserved from yeast to humans and is now linked to a variety of different cellular regulatory functions. Ubiquitin can be covalently attached to other proteins to signal targeted degradation (*1*), endocytic sorting (*2*, *3*), transcriptional activation and repression (*4*, *5*), and budding of retroviral virions (*6*). The outcome of ubiquitylation depends on how many ubiquitin moieties are attached and through which lysine residue these moieties are linked.

Covalent attachment of ubiquitin occurs via an enzyme cascade, which begins with a thioester bond between the C-terminal glycine of ubiquitin and a catalytic cysteine of an E1 ubiquitin activating enzyme (*7*, *8*). Ubiquitin is then passed to an E2 ubiquitin conjugating enzyme, which may catalyze the formation of an isopeptide bond between ubiquitin and a protein substrate or transfer ubiquitin to an E3 ubiquitin protein ligase to perform this function. The cycle is repeated to form polyubiquitin chains, the most well studied being K48-linked chains, which serve as a signal for recognition by the 26S proteasome, resulting in substrate proteolysis (*9*, *10*).

A large number of ubiquitin receptors have been identified, and three ubiquitin binding families have emerged, including ubiquitin-associated (UBA)[1] domains (*11*, *12*), ubiquitin interacting motifs (UIM) (*13*), and coupling of ubiquitin conjugation to ER degradation (CUE) domains (*14*, *15*). The structures of two CUE domain−ubiquitin complexes have recently been determined, one involving the yeast Cue2 protein determined by NMR (*16*) and the other involving the CUE domain of Vps9p determined by X-ray crystallography (*17*). Interestingly, whereas the yeast Cue2 CUE domain binds ubiquitin as a monomer, the Vps9p CUE domain functions as a dimer *in vivo* and undergoes domain swapping to form a dimer interface that is required for high-affinity ubiquitin binding (*17*).

The DNA repair protein hHR23a has two UBA domains, and the structure of each of them has been determined separately (*18*, *19*) and within the context of the full-length protein (*20*). These domains are reported to bind ubiquitin in yeast (*11*, *12*) and in humans (*21*), and hHR23a can mitigate the degradation of other proteins by binding ubiquitin and inhibiting polyubiquitin chain formation (*21*, *22*). The interaction of the UBA domains with ubiquitin has not yet been well characterized, although in the yeast homologue Rad23, a single amino acid substitution in each of the UBA domains (corresponding to L198A and L355A in hHR23a) destroys binding to ubiquitin (*11*, *23*).

Interestingly, hHR23a also binds S5a (*24*) and S2 (in yeast) (*25*), which are components of the 26S proteasome. Thus, it has been hypothesized that hHR23a may link ubiquitylation and the proteasome (*23*, *26*), although whether hHR23a can simultaneously bind S5a and ubiquitin has not yet been determined. HHR23a binds S5a through the ubiquitin-like (UBL) domain (*24*). Indeed, a number of proteins that contain

† This work was in part funded by the Minnesota Medical Foundation (K.J.W.), an American Cancer Society Institutional Grant (K.J.W.), National Institutes of Health Grants CA097004-01A1 (K.J.W.) and CA37-CA64888 (P.M.H.), and a scholarship from the Agency for Science, Technology and Research of Singapore (A.M.G.).

* To whom correspondence should be addressed. E-mail: walte048@umn.edu.

‡ University of Minnesota.

§ Harvard Medical School.

[1] Abbreviations: CUE, coupling of ubiquitin conjugation to ER degradation; hHR23, human homologue of Rad23; HSQC, heteronuclear single-quantum coherence; NER, nucleotide excision repair; NMR, nuclear magnetic resonance; NOE, nuclear Overhauser effect; UBA, ubiquitin-associated; UBL, ubiquitin-like; UIM, ubiquitin interacting motif.

10.1021/bi035391j CCC: $25.00
Published on Web 10/29/2003

both UBL and UBA domains have now been identified, and intramolecular interactions between UBL and UBA domains have been shown for hHR23a (*20*) and hHR23b (*27*). UBL domain binding to the UBA domains and to S5a, however, is mutually exclusive, and hHR23a loses its interdomain structure as a result of S5a binding (*20*).

Here we describe the hHR23a−ubiquitin contact surface and describe how ubiquitin regulates hHR23a protein structure. In addition, we find that the UBA domains of an hHR23a mutant (L198A/L355A), based on mutations identified in the yeast Rad23 homologue as deficient in ubiquitin binding (*11*, *23*), are unstructured. Finally, we examine whether hHR23a can link ubiquitin to S5a by forming a ternary complex.

MATERIALS AND METHODS

Preparation of NMR Samples. HHR23a, hHR23a(L198A/L355A), and the single-domain construct of the UBA1 domain (UBA1) (C&P Biotech Corp.) were each cloned into the pGEX-6p expression vector in frame with the glutathione *S*-transferase (GST) fusion protein. Protein expression was induced in BL21(DE3) cells with 0.4 mM isopropyl β-D-thiogalactoside (IPTG) at 37 °C. After affinity purification on glutathione−Sepharose resin, the protein of interest was separated from the GST tag by cleavage with PreScission protease. Further purification was achieved on an FPLC system (Pharmacia), using either Superdex 200 [for hHR23a and hHR23a(L198A/L355A)] or 75 (for UBA1) preparative columns.

P. Young generously provided us with a plasmid for the expression of S5a(196−307) (*13*). Ubiquitin and UBA2 were cloned into a pET expression vector in frame with a polyhistidine tag and expressed in BL21(DE3) cells in the same way as the GST fusion proteins. For both of these proteins, the presence of a polyhistidine tag enabled purification because it binds to Ni−NTA resin and elutes with 0.25 M imidazole. Further purification was accomplished by FPLC. Unlabeled ubiquitin was purchased (Sigma-Aldrich).

For all of the proteins studied here, we were able to produce labeled samples for NMR spectroscopy, by growth and expression in M9 minimal medium with $^{15}NH_4Cl$ as the only source of nitrogen.

NMR Spectroscopy. All NMR samples were dissolved in 20 mM $NaPO_4$ (pH 6.5), 100 mM NaCl, 0.1% NaN_3, and 10% D_2O. All spectra were acquired at 25 °C on a Varian 800 MHz NMR spectrometer. All spectra were processed using NMRPipe (*28*) and visualized in XEASY (*29*). Intermolecular NOE interactions between hHR23a and ubiquitin were obtained by acquiring an ^{15}N-dispersed NOESY spectrum on a sample containing ^{2}H- and ^{15}N-labeled hHR23a and unlabeled ubiquitin at a 1:3 molar ratio. In such a spectrum, all amide to aliphatic NOE cross-peaks are exclusively intermolecular (*30*). This experiment was carried out with a mixing time of 200 ms.

Titration Experiments for Mapping the hHR23a−Ubiquitin Contact Surface. To characterize the interaction with ubiquitin, an NMR titration study was performed where the $^{1}H-^{15}N$ HSQC spectrum of ^{15}N-labeled hHR23a was monitored upon addition of increasing quantities of unlabeled ubiquitin. Concentrations were calculated by using extinction coefficients based on amino acid composition. The absorbance at 280 nm was measured for each protein in urea, and the concentration of hHR23a used in the $^{1}H-^{15}N$ HSQC experiments was 0.2 mM. The change in the chemical shift of the amide nitrogen and proton atoms was measured through $^{1}H-^{15}N$ HSQC spectra and treated according to eq 1.

$$\sqrt{0.2\Delta\delta_N{}^2 + \Delta\delta_H{}^2} \quad (1)$$

In this equation, $\Delta\delta_N$ and $\Delta\delta_H$ represent the changes in nitrogen and proton chemical shifts (in parts per million), respectively.

Similarly, to characterize the UBA domain interaction surface of ubiquitin, an NMR titration study was performed where the $^{1}H-^{15}N$ HSQC spectrum of ^{15}N-labeled ubiquitin was monitored upon addition of increasing quantities of unlabeled UBA1 or UBA2. For the hHR23a−ubiquitin−S5a(196−307) ternary complex, we added S5a(196−307) to a sample containing 0.2 mM hHR23a and 0.5 mM ubiquitin in 1 mM DTT, 20 mM $NaPO_4$ (pH 6.5), and 100 mM NaCl. A $^{1}H-^{15}N$ HSQC spectrum was acquired at a 1:2.5:1 hHR23a:ubiquitin:S5a(196−307) molar ratio.

NMR Dynamics Studies. Rates for ^{15}N longitudinal [$R_N(N_Z)$] and transverse [$R_N(N_X)$] relaxation and magnitudes of the heteronuclear NOE enhancements were recorded on hHR23a in complex with ubiquitin. These data were collected at 800 MHz, 25 °C, and pH 6.5 on 0.2 mM hHR23a−ubiquitin protein complex at a 1:2.5 molar ratio. In the hHR23a−ubiquitin complex, hHR23a was ^{15}N-labeled and ubiquitin was unlabeled. $R_N(N_Z)$ and $R_N(N_X)$ were derived by fitting data acquired with different relaxation delays to a single-exponential decay function, and error values were determined by repeating one data point. Two spectra were recorded for steady-state NOE intensities, one with a 4 s proton saturation to achieve the steady-state intensity and the other as a control spectrum with no saturation to obtain the Zeeman intensity. The process for the control spectrum was repeated to determine error values. The heteronuclear NOE enhancements (XNOE) were then calculated from the ratio described in eq 2.

$$\mathrm{XNOE} = \left|\left(\frac{\gamma_H}{\gamma_N}\right)\left[\frac{R_N(H_Z^N \leftrightarrow N_Z)}{R_N(N_Z)}\right]\right| \quad (2)$$

RESULTS

The UBL Domain Experiences Chemical Shift Changes when the UBA Domains Bind Ubiquitin. HHR23a contains an internal UBA domain and C-terminal UBA domain that compete for binding to an N-terminal UBL domain (*20*). The UBA domains also bind ubiquitin (*11*, *12*). We have used NMR spectroscopy to map the ubiquitin recognition surface on hHR23a. Initially, we conducted $^{1}H-^{15}N$ HSQC experiments to test for binding. We carried out $^{1}H-^{15}N$ HSQC experiments with ^{15}N-labeled hHR23a alone and with increasing quantities of ubiquitin (Figure 1A).

To illustrate how each domain in hHR23a is affected by ubiquitin binding, we have mapped the amide nitrogen and hydrogen chemical shift changes for each residue according to eq 1, as described in Materials and Methods. This information can be used to map binding surfaces, as the frequency at which an atom resonates is sensitive to its

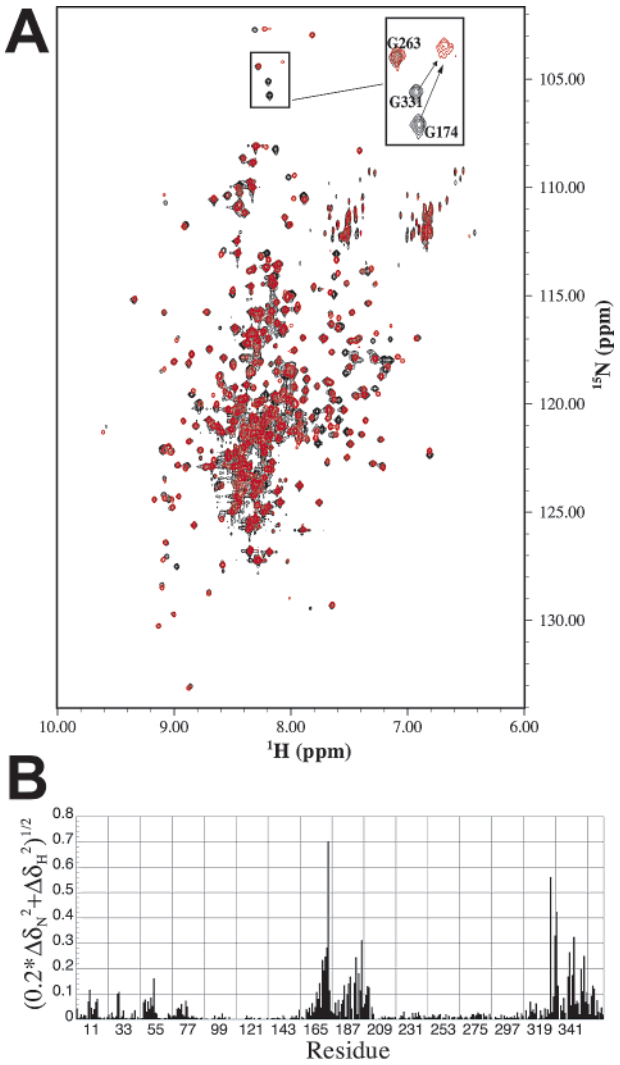

FIGURE 1: UBA domains of hHR23a bind ubiquitin. (A) ^{1}H−^{15}N HSQC spectrum of hHR23a alone (black) and at a molar ratio of 1:2.5 with ubiquitin (red). In the expanded region, an example of the large chemical shift changes observed in the UBA domains is depicted for two glycine residues. (B) Chemical shift perturbation data treated according to eq 1, as described in Materials and Methods.

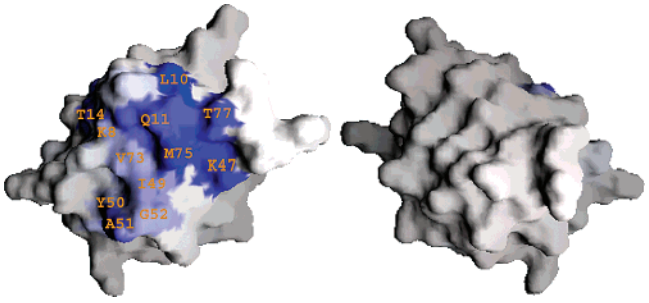

FIGURE 2: UBA domain binding surface of the UBL domain that undergoes chemical shift changes when hHR23a binds ubiquitin. The program GRASP (*34*) was used to generate this figure, and the structure on the right is rotated 180° relative to that on the left. The reported UBL domain coordinates for hHR23a were used to generate this figure (*20*).

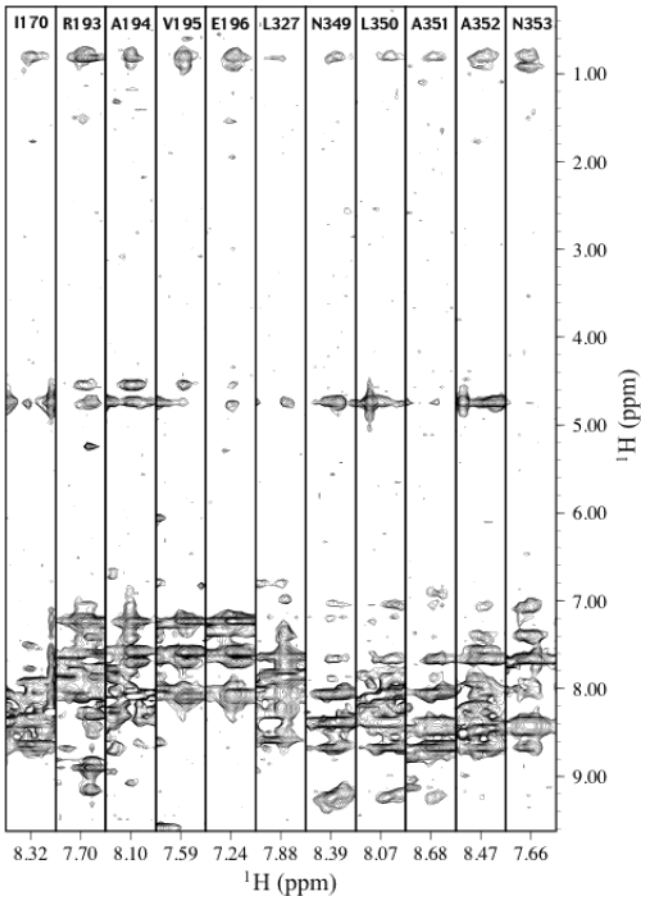

FIGURE 3: Residues in α1 and α3 of UBA1 and UBA2 have intermolecular NOE interactions with ubiquitin. ^{15}N planes were selected for each region showing amide−aliphatic NOEs. NOEs between amide protons are both inter- and intramolecular, and H_2O appears at 4.8 ppm.

chemical environment. These values are provided in Figure 1B, and clearly, the largest chemical shift perturbations appear in the UBA domains. This finding is consistent with ubiquitin recognition occurring in the UBA domains.

The XPC binding domain of hHR23a does not experience significant chemical shift changes when the UBA domains bind ubiquitin. However, resonances in the UBL domain are shifted by hHR23a binding ubiquitin. We have mapped the values of Figure 1B for the UBL domain onto a surface diagram (Figure 2). In previous work, we found that the UBL domain contacts each of the hHR23a UBA domains (*20*) and those residues of the UBL domain that are perturbed by ubiquitin binding indeed reside in the UBA contact surface. Hence, we hypothesize that the chemical shift changes observed in the UBL domain are due to a change in hHR23a protein structure.

Ubiquitin Binds a Surface Formed by α1 and α3 of the UBA Domains. To determine unambiguously the ubiquitin contact surface of hHR23a, we acquired a ^{15}N-dispersed NOESY spectrum on ^{15}N- and ^{2}H-labeled hHR23a and unlabeled ubiquitin. In such a spectrum, all cross-peaks between amide and aliphatic protons must be between hHR23a and ubiquitin. Figure 3 includes selected nitrogen planes of amide resonances that contain NOE interactions with aliphatic protons. These residues are predominately contained within α1 and α3 of UBA1 and UBA2. Indeed, no residue in the UBL domain has such intermolecular NOE interactions. This finding further suggests that the observed chemical shift changes in the UBL domain are due to changes in hHR23a protein structure.

In Figure 4, we present the ubiquitin recognition surface of each UBA domain by depicting in color those residues

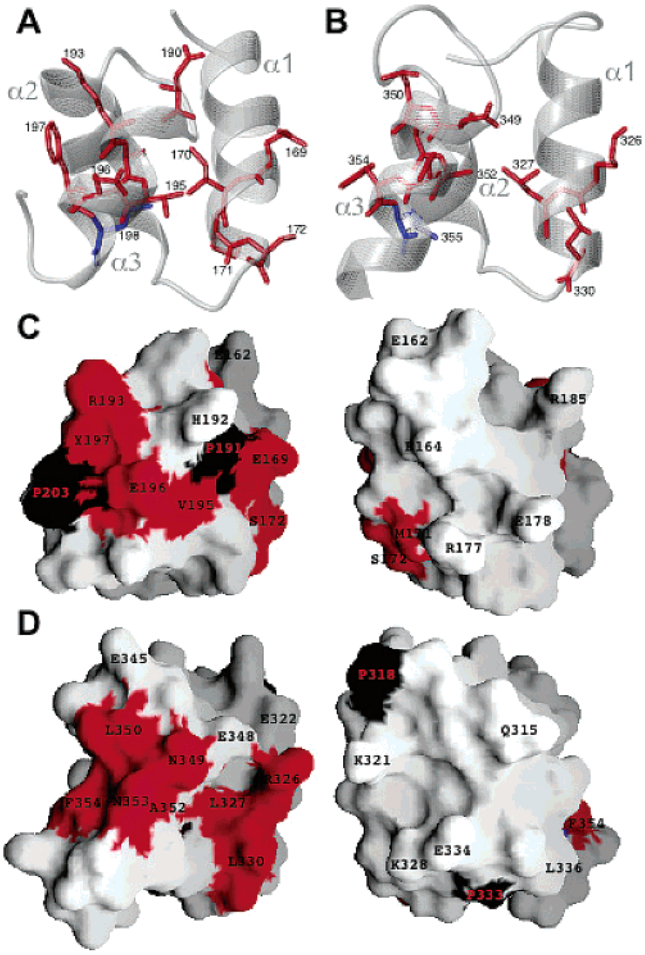

FIGURE 4: UBA1 and UBA2 use an analogous ubiquitin recognition surface. Panels A and B show the secondary structure diagrams of UBA1 and UBA2, respectively, such that the backbone atoms of α1 and α3 of UBA2 are superimposed onto the analogous atoms in UBA1. Residues with NOEs to ubiquitin are shown in red, and L198 and L355 are highlighted in blue. In panels C and D, surface diagrams of UBA1 and UBA2, respectively, are shown with those residues showing intermolecular NOEs colored red. Prolines, which lack amide protons, are colored black. The structures on the right are rotated 180° relative to those on the left, which are in the same orientation as the structures in panels A and B. The program MOLMOL (*35*) was used to generate panels A and B, and GRASP (*34*) was used to generate panels C and D. The reported UBA domain coordinates for hHR23a were used to generate this figure (*20*).

that have intermolecular NOE interactions. Proline residues are displayed in black as they lack amide protons, and we are therefore unable to determine whether they contact ubiquitin by using this experiment. The ubiquitin recognition surface of each UBA domain is largely hydrophobic with negatively charged regions (Figure 5). Interestingly, the CUE domain of the yeast CUE2 protein uses an analogous ubiquitin recognition surface, which is predominately hydrophobic (*16*).

Single-Amino Acid Substitutions in the UBA Domains Disrupt Their Fold. Studies in yeast identified a Rad23 mutant that is defective for ubiquitin binding (*11*, *23*). On the basis of these studies, we generated an analogous hHR23a protein construct in which L198 of UBA1 and L355 of UBA2 are substituted with alanine. The side chains of each of these leucine residues are directed toward the protein interior (Figure 4), and these residues are therefore more

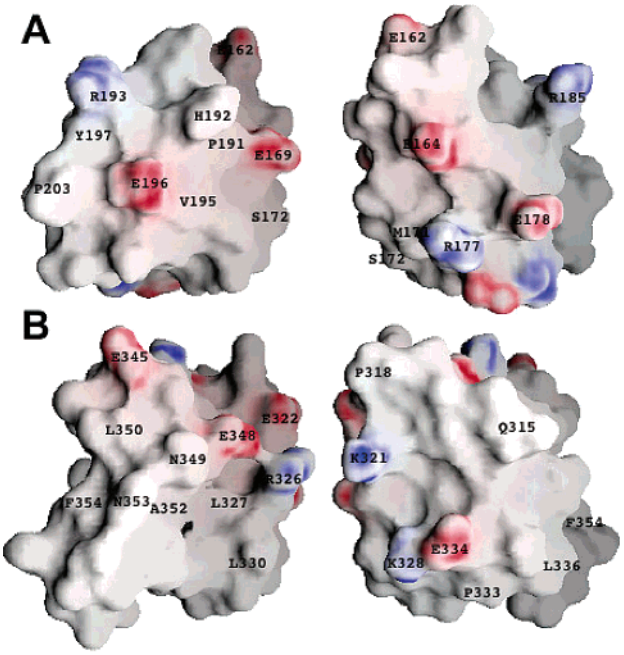

FIGURE 5: Electrostatic surface diagrams of UBA1 (A) and UBA2 (B) reveal that the ubiquitin recognition surfaces are predominately hydrophobic with acidic regions. The orientation of these figures is identical to that of panels C and D of Figure 4. This figure was generated by using GRASP (*34*) and the coordinates of UBA1 and UBA2 as solved in the full-length hHR23a protein (*20*).

likely to be important for overall UBA domain structure than for binding ubiquitin (*11*). To test this hypothesis, we acquired a $^{1}H-^{15}N$ HSQC spectrum of the ^{15}N-labeled hHR23a(L198A/L355A) mutant. In this hHR23a mutant construct, the resonances originating from residues in the UBA domains lose their chemical shift dispersion (data not shown), which is characteristic of randomly coiled peptides. We tested this construct for ubiquitin binding and found it to be defective (data not shown).

Ubiquitin Binds Each UBA Domain of hHR23a with an Almost Identical Surface. To determine how the UBA domains of hHR23a are recognized by ubiquitin, we acquired a $^{1}H-^{15}N$ HSQC spectrum of ^{15}N-labeled ubiquitin alone and with increasing quantities of unlabeled UBA1 or UBA2. In these experiments, each UBA domain is expressed as a single-domain construct. As expected, addition of either UBA domain produces chemical shift changes in the $^{1}H-^{15}N$ HSQC spectrum of ubiquitin. The measured chemical shift perturbations of ubiquitin amide resonances at equimolar concentrations with either UBA domain were treated according to eq 1. The results were then mapped onto the surface diagram of ubiquitin (Figure 6).

The UBA1 and UBA2 interaction surfaces on ubiquitin are provided in panels A and B of Figure 6, respectively. The electrostatic properties of this surface, which contains hydrophobic and positively charged residues, are complementary to those of the ubiquitin binding surface of the UBA domains. This surface is analogous to the UBA binding surface of the hHR23a UBL domain and is formed by β-strands. K48 of ubiquitin is within the UBA contact surface, consistent with the finding that hHR23a blocks K48-linked ubiquitin chain formation (*21*).

Ubiquitin Binding Disrupts the hHR23a UBL Domain−UBA Domain Interaction. To test our hypothesis that the

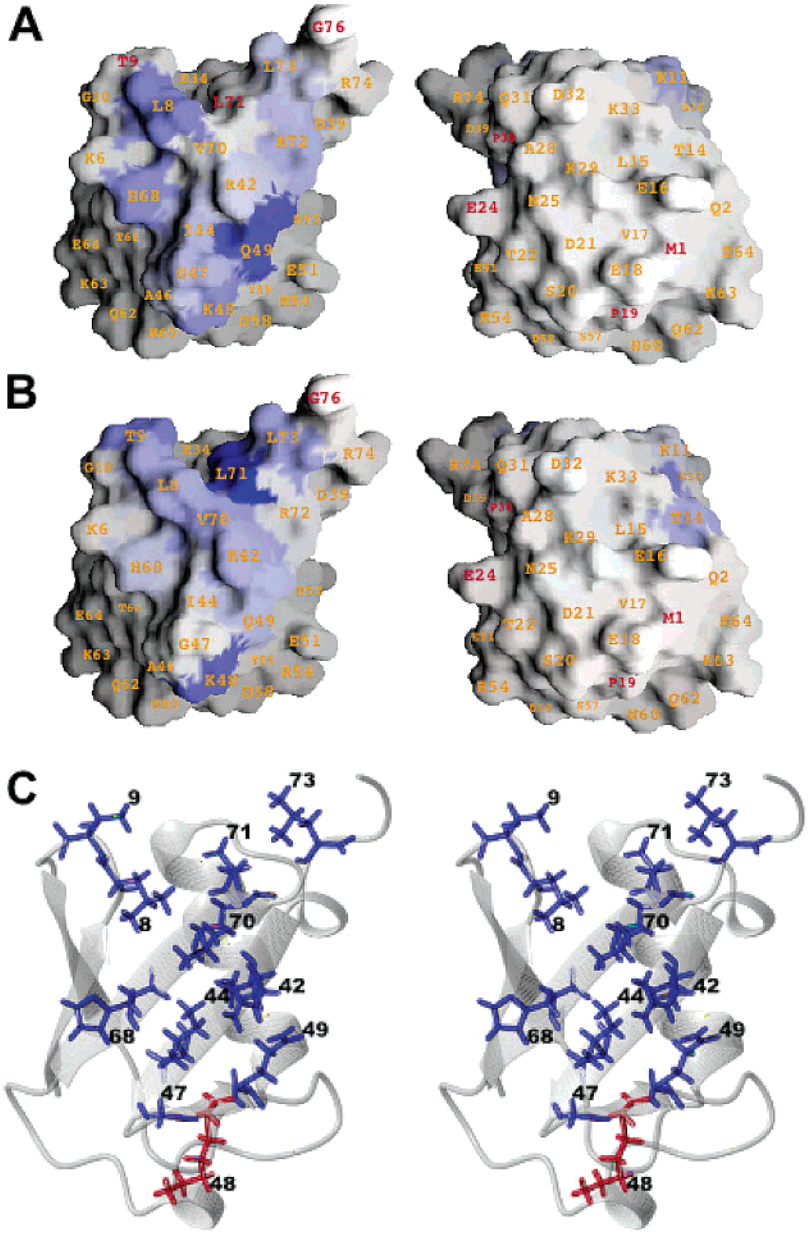

FIGURE 6: UBA1 (A) and UBA2 (B) bind the surface on ubiquitin that is formed by β-strands and includes K48. Panels A and B were made by mapping the chemical shift perturbations observed in the $^{1}H-^{15}N$ HSQC spectrum of ^{15}N-labeled ubiquitin from adding equimolar quantities of UBA1 (A) and UBA2 (B). Residues labeled red, including prolines and those lacking chemical shift assignments, were omitted from this analysis. Resonances originating from T9 and L71 disappear from the spectrum upon addition of UBA1. For clarity in panel C, a stereoview of the secondary structure of ubiquitin is provided whereby residues that experienced chemical shift changes in the presence of either UBA domain are displayed in blue and K48 is highlighted in red. The orientation of the structure displayed in panel C is identical to that shown on the left side of panels A and B. The reported ubiquitin coordinates were used to generate this figure (*36*).

observed chemical shift changes in the UBL domain originate from changes in hHR23a structure, we performed ^{15}N NMR relaxation experiments on the hHR23a−ubiquitin complex at a molar ratio of 1:2.5 (Figure 7). These experiments probe the internal dynamics of each residue and can be used to identify flexible regions within a protein and to assess how each domain tumbles. In the unbound hHR23a protein, the relaxation data reflect the UBL domain−UBA domain interaction by fast $R_N(N_X)$ relaxation values (*20*).

When in complex with ubiquitin, as in the free protein, the linker regions connecting each of the four structured domains of hHR23a have fast $R_N(N_Z)$, slow $R_N(N_X)$, and large heteronuclear NOE enhancements. Such trends indicate flexibility, and in fact, the values in these regions change little upon addition of ubiquitin. In contrast, the $R_N(N_X)$ relaxation values for residues in the UBL domain decreased substantially compared to their values in the free protein (Table 1), indicating that this domain is tumbling in a more labile manner when hHR23a is bound to ubiquitin (*20*). This finding supports our hypothesis that ubiquitin binding to UBA domains precludes UBL binding.

HHR23a Can Simultaneously Bind Ubiquitin and S5a. We tested whether hHR23a can link ubiquitin to S5a by forming a ternary complex. We used an S5a construct that spans residues M196−D307 [S5a(196−307)]. This construct contains two UIMs and was previously shown to bind hHR23a with an affinity equal to that of the full-length S5a protein (*24*). We acquired a $^{1}H-^{15}N$ HSQC spectrum of ^{15}N-labeled hHR23a with ubiquitin and S5a at a molar ratio of 1:2.5:1. Indeed, we observed chemical shift perturbations consistent

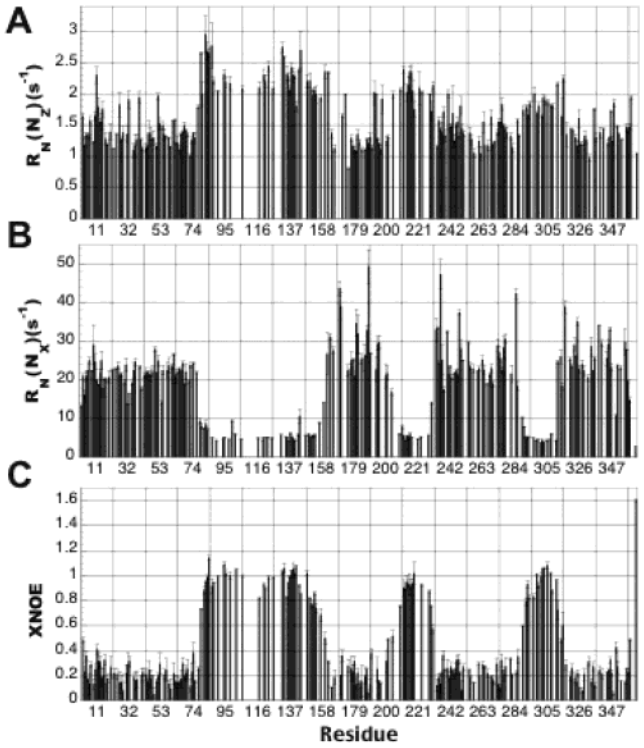

FIGURE 7: hHR23a protein structure is altered by ubiquitin. Rates for ^{15}N longitudinal [$R_N(N_Z)$] (A) and transverse [$R_N(N_X)$] (B) relaxation and magnitudes of the heteronuclear NOE enhancements (C) for the hHR23a−ubiquitin complex at a 1:2.5 molar ratio reveal a loss of domain interaction. These data were collected at 800 MHz, 25 °C, and pH 6.5.

Table 1: Average Relaxation Values for Each Domain of hHR23a Alone (*20*) and in Complex with Ubiquitin

	T_1 (s^{-1})		T_2 (s^{-1})		XNOE	
domain	free	complex	free	complex	free	complex
UBL	1.2	1.4	41.9	22.0	0.2	0.2
UBA1	1.4	1.3	27.9	27.8	0.2	0.2
XPC binding	1.3	1.4	35.0	25.6	0.2	0.2
UBA2	1.4	1.4	30.0	25.6	0.3	0.2

with the UBL domain binding S5a and the UBA domains binding ubiquitin. Figure 8A reveals chemical shift perturbation analysis in accordance with eq 1. Hence, hHR23a can link ubiquitin to S5a (Figure 8B).

DISCUSSION

HHR23a is a member of a class of UBL/UBA proteins and has a UBL domain that binds S5a (*24*) and UBA domains that bind ubiquitin (*11*, *12*). Here we report that α1 and α3 of UBA1 and UBA2 form a predominately hydrophobic surface that is used to bind ubiquitin. NOE interactions with residues in α3 are stronger than those involving residues in α1, and it is in fact α3 that forms the UBL contact surface (*20*). Interestingly, the surface of ubiquitin that we identified here for binding UBA also binds UIMs (*31*) and CUE domains of Vps9p (*17*) and yeast CUE2 (*16*), which suggests that each of these three motifs competes for monoubiquitin binding. However, it is also possible that individual domains behave cooperatively in binding polyubiquitin chains. Indeed, an hHR23a construct containing both of the UBA domains affords stronger binding to K48-linked tetraubiquitin than do those containing only one UBA domain (*21*).

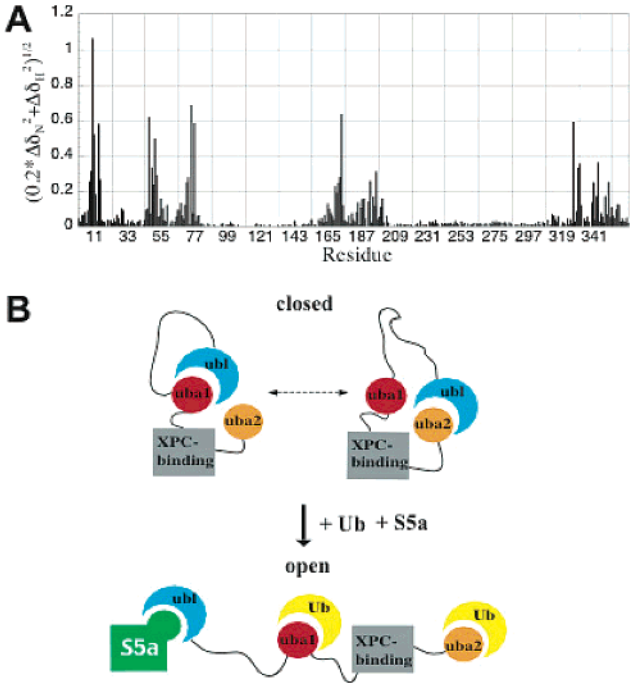

FIGURE 8: hHR23a links ubiquitin and S5a. Chemical shift perturbation analysis reveals that hHR23a simultaneously binds ubiquitin and S5a (A). This plot contains the amide chemical shift changes treated according to eq 1 for the hHR23a−ubiquitin−S5a complex at a 1:2.5:1 molar ratio. The schematic in panel B models how hHR23a links ubiquitin and S5a.

The recently determined structures of two ubiquitin−CUE domain complexes reveal two mechanisms of ubiquitin recognition. The crystal structure of the CUE domain of Vps9p reveals that it undergoes domain swapping to form a dimer, which allows for high-affinity binding to ubiquitin (*17*). In this complex, ubiquitin interacts with L427 and V431 of α2. In contrast, in the CUE−ubiquitin complex determined by NMR, the CUE domain recognizes ubiquitin as a monomer through contacts with α1 and α3 (*16*). In addition to hHR23a, many other proteins contain more than one UBA domain (such as NUB1), and it is therefore conceivable that such proteins could undergo domain swapping. Our studies with hHR23a, however, support a binding mechanism similar to that used by CUE2, namely, that hHR23a recognizes ubiquitin through contacts with α1 and α3 of each UBA domain.

The UBA domain binding surface of ubiquitin is formed by β-strands and includes K48. This presence of K48 on the binding surface explains how hHR23a inhibits K48-linked polyubiquitin chain formation (*21*, *22*). K29- and K63-linked polyubiquitin chain formation is not inhibited by hHR23a (*21*), and indeed, each of those residues is remote from the UBA binding surface. Interestingly, hHR23a preferentially binds K48-linked polyubiquitin chains over those linked via K29 or K63, and this preference may exist because chains linked by K48 provide consecutive UBA binding patches that are simultaneously contacted by each of the hHR23a UBA domains (*21*).

Ubiquitin binding causes a change in hHR23a structure as an analogous region on the UBL domain surface also contacts UBA1 and UBA2. Indeed, an hHR23a construct in which the UBL domain is deleted is suggested to bind polyubiquitin chains with higher affinity than the native

protein (*21*). Therefore, it is likely that S5a enhances the binding of hHR23a to polyubiquitin chains and vice versa, which implies that S5a and hHR23 proteins could function synergistically to promote substrate proteolysis by recruiting certain polyubiquitinated substrates to the proteasome. Indeed, a yeast strain lacking both Rad23 and Rpn10 has increased levels of multiubiquitinated proteins (*32*).

We have found that S5a(196−307) can bind the hHR23a−ubiquitin complex and, therefore, that hHR23a may functionally link ubiquitin with S5a and the proteasome. Here we used a truncated S5a construct but expect that this construct is representative of the full-length protein for the following reasons. First, S5a(196−307) and full-length S5a (*20*, *33*) bind to the same region on hHR23a, namely, the β-strand surface of the UBL domain. Second, the presence of an 80-residue flexible linker separating the UBL domain from UBA1 and our findings that hHR23a lacks interdomain interactions when complexed with ubiquitin remove the concern that the full-length protein may experience steric limitations not present for S5a(196−307). Future experiments are needed, however, to test whether hHR23a and S5a bind polyubiquitin chains cooperatively.

ACKNOWLEDGMENT

We are grateful to Dr. Patrick Young for generously providing us with the S5a(196−307) plasmid. NMR data were acquired at the NMR facility of the University of Minnesota, and we thank Dr. David Live and Dr. Beverly Ostrowsky for their technical assistance. NMR instrumentation was provided with funds from the National Science Foundation (Grant BIR-961477), the University of Minnesota Medical School, and the Minnesota Medical Foundation. Data processing and structure calculations were performed in the Basic Sciences Computing Lab of the University of Minnesota Supercomputing Institute.

REFERENCES

1. Coux, O., Tanaka, K., and Goldberg, A. L. (1996) *Annu. Rev. Biochem. 65*, 801−847.
2. Hicke, L. (2001) *Cell 106*, 527−530.
3. Katzmann, D. J., Odorizzi, G., and Emr, S. D. (2002) *Nat. Rev. Mol. Cell Biol. 3*, 893−905.
4. Conaway, R. C., Brower, C. S., and Conaway, J. W. (2002) *Science 296*, 1254−1258.
5. Muratani, M., and Tansey, W. P. (2003) *Nat. Rev. Mol. Cell Biol. 4*, 192−201.
6. Pornillos, O., Garrus, J. E., and Sundquist, W. I. (2002) *Trends Cell Biol. 12*, 569−579.
7. Ciechanover, A. (1994) *Cell 79*, 13−21.
8. Hochstrasser, M. (1996) *Annu. Rev. Genet. 30*, 405−439.
9. Chau, V., Tobias, J. W., Bachmair, A., Marriott, D., Ecker, D. J., Gonda, D. K., and Varshavsky, A. (1989) *Science 243*, 1576−1583.
10. Finley, D., Sadis, S., Monia, B. P., Boucher, P., Ecker, D. J., Crooke, S. T., and Chau, V. (1994) *Mol. Biol. Cell 14*, 5501−5509.
11. Bertolaet, B. L., Clarke, D. J., Wolff, M., Watson, M. H., Henze, M., Divita, G., and Reed, S. I. (2001) *Nat. Struct. Biol. 8*, 417−422.
12. Chen, L., Shinde, U., Ortolan, T. G., and Madura, K. (2001) *EMBO Rep. 2*, 933−938.
13. Young, P., Deveraux, Q., Beal, R. E., Pickart, C. M., and Rechsteiner, M. (1998) *J. Biol. Chem. 273*, 5461−5467.
14. Donaldson, K. M., Yin, H., Gekakis, N., Supek, F., and Joazeiro, C. A. (2003) *Curr. Biol. 13*, 258−262.
15. Shih, S. C., Prag, G., Francis, S. A., Sutanto, M. A., Hurley, J. H., and Hicke, L. (2003) *EMBO J. 22*, 1273−1281.
16. Kang, R. S., Daniels, C. M., Francis, S. A., Shih, S. C., Salerno, W. J., Hicke, L., and Radhakrishnan, I. (2003) *Cell 113*, 621−630.
17. Prag, G., Misra, S., Jones, E. A., Ghirlando, R., Davies, B. A., Horazdovsky, B. F., and Hurley, J. H. (2003) *Cell 113*, 609−620.
18. Dieckmann, T., Withers-Ward, E. S., Jarosinski, M. A., Liu, C. F., Chen, I. S., and Feigon, J. (1998) *Nat. Struct. Biol. 5*, 1042−1047.
19. Mueller, T. D., and Feigon, J. (2002) *J. Mol. Biol. 319*, 1243−1255.
20. Walters, K. J., Lech, P. J., Goh, A. M., Wang, Q., and Howley, P. M. (2003) *Proc. Nat. Acad. Sci. 100*, 12694−12699.
21. Raasi, S., and Pickart, C. M. (2003) *J. Biol. Chem. 278*, 8951−8959.
22. Ortolan, T. G., Tongaonkar, P., Lambertson, D., Chen, L., Schauber, C., and Madura, K. (2000) *Nat. Cell Biol. 2*, 601−608.
23. Chen, L., and Madura, K. (2002) *Mol. Cell. Biol. 22*, 4902−4913.
24. Hiyama, H., Yokoi, M., Masutani, C., Sugasawa, K., Maekawa, T., Tanaka, K., Hoeijmakers, J. H., and Hanaoka, F. (1999) *J. Biol. Chem. 274*, 28019−28025.
25. Elsasser, S., Gali, R. R., Schwickart, M., Larsen, C. N., Leggett, D. S., Muller, B., Feng, M. T., Tubing, F., Dittmar, G. A., and Finley, D. (2002) *Nat. Cell Biol. 4*, 725−730.
26. Walters, K. J., Goh, A. M., Wang, Q., Wagner, G., and Howley, P. M. (2003) *BBA* (in press).
27. Ryu, K. S., Lee, K. J., Bae, S. H., Kim, B. K., Kim, K. A., and Choi, B. S. (2003) *J. Biol. Chem. 278*, 36621−36627.
28. Delaglio, F., Grzesiek, S., Vuister, G. W., Zhu, G., Pfeifer, J., and Bax, A. (1995) *J. Biomol. NMR 6*, 277−293.
29. Bartels, C., Xia, T.-H., Billeter, M., Güntert, P., and Wüthrich, K. (1995) *J. Biomol. NMR 6*, 1−10.
30. Walters, K. J., Matsuo, H., and Wagner, G. (1997) *J. Am. Chem. Soc. 119*, 5958−5959.
31. Fischer, R. D., Wang, B., Alam, S. L., Higginson, D. S., Robinson, H., Sundquist, W. I., and Hill, C. P. (2003) *J. Biol. Chem. 278*, 28976−28984.
32. Lambertson, D., Chen, L., and Madura, K. (1999) *Genetics 153*, 69−79.
33. Walters, K. J., Kleijnen, M. F., Goh, A. M., Wagner, G., and Howley, P. M. (2002) *Biochemistry 41*, 1767−1777.
34. Nicholls, A. J. (1993) *GRASP Manual*, Columbia University, New York.
35. Koradi, R., Billeter, M., and Wüthrich, K. (1996) *J. Mol. Graphics 14*, 51−55.
36. Ramage, R., Green, J., Muir, T. W., Ogunjobi, O. M., Love, S., and Shaw, K. (1994) *Biochem. J. 299* (Part 1), 151−158.

BI035391J